

UC San Diego

UC San Diego Previously Published Works

Title

Investigation of a field-scale energy micropile in stratified soil under cyclic temperature changes

Permalink

<https://escholarship.org/uc/item/7hh1z63k>

Authors

Casagrande, Brunella
Saboya, Fernando
McCartney, John S
[et al.](#)

Publication Date

2022-03-01

DOI

10.1016/j.gete.2021.100263

Peer reviewed

1 **Investigation of a Field-Scale Energy Micropile in Stratified**
2 **Soil under Cyclic Temperature Changes**

3
4 **Brunella Casagrande Brunelli Santos**

5 MSc – State University of Northern Fluminense Darcy Ribeiro - UENF
6 Department of Civil Engineering, Campos dos Goytacazes, Rio de Janeiro, Brazil.
7 brunellacasagrandeb@gmail.com

8
9 **Fernando Saboya Jr.**

10 Professor – State University of Northern Fluminense Darcy Ribeiro - UENF
11 Department of Civil Engineering, Campos dos Goytacazes, Rio de Janeiro, Brazil.
12 saboya@uenf.br.

13
14 **John S. McCartney**

15 Professor and Department Chair - University of California San Diego - UCSD
16 Department of Structural Engineering. La Jolla, CA, USA.
17 mccartney@ucsd.edu

18
19 **Sérgio Tibana**

20 Professor – State University of Northern Fluminense Darcy Ribeiro - UENF
21 Department of Civil Engineering, Campos Rio de Janeiro, Brazil.
22 tibana@uenf.br

23 **Abstract:** Data regarding energy pile behavior in tropical climate regions is not as readily
24 available as in temperate climate regions, which are generally heating dominated (i.e.,
25 focused on extracting heat from a relatively cool subsurface). Further, there has not been
26 a major effort to understand the behavior of micropiles converted into energy piles, which
27 may have different behavior from other energy piles due to the disturbance associated
28 with installation, especially at the toe. This paper presents the results of a series of
29 thermal response tests (TRTs) on a 12 m-long instrumented energy micropile installed in
30 a sedimentary tropical soil to understand the impacts of heating and cooling cycles.
31 Vibrating wire strain gauges embedded within the energy micropile were used to assess
32 the mechanical performance of the pile when subject to changes in temperature. Results
33 indicate that the temperature distribution with depth and the resulting thermal axial strains
34 are strongly dependent on the subsoil stratigraphy and are far from being homogeneous
35 along the length of the pile. In particular, the temperature gradients across interfaces with
36 an organic clay deposit were found to have a major effect on the thermal axial strains.
37 Hysteresis in the thermal axial strains during the process of heating and cooling was also
38 analyzed and was found to represent a diminishing effect on the mobilized coefficient of
39 thermal expansion with each cycle.

40 **Keywords:** Energy Piles, Thermo-Mechanical Hysteresis, Thermal Response Test.

41 Introduction

42 While energy is essential to enable the socio-economic development of society, it
43 represents a segment having one of the most adverse impacts on the environment.
44 According to the Global Carbon Budget (2018), carbon dioxide is the gas that contributes
45 58.8% to the greenhouse effect. Geothermal heat exchange contributes to the reduction
46 in CO₂ emissions through more efficient use of electricity when providing heating and
47 cooling. Geothermal heat exchange can be used in any location and at any time of the
48 year. In order to access geothermal energy in the shallow surface, energy piles are often
49 used to exchange heat between a building and the subsurface using a ground-source
50 heat pump (GSHP) (Brandl 2006; Laloui et al. 2006; Bourne-Webb et al. 2009).

51 Energy piles support buildings while acting as underground heat exchangers using
52 closed-loop, flexible, high-density polyethylene (HDPE) tubing within the reinforcing cage,
53 through which a heat carrier fluid is circulated to maintain thermal comfort the building.
54 The temperature of the fluid is controlled using a heat pump within the building. During
55 heating and cooling cycles, energy piles expand and contract volumetrically which may
56 be restrained by pile–soil interaction (Laloui et al. 2006; Amatya et al. 2012; Chen et al.
57 2016; Faizal et al. 2018). In some cases, this may result in unwanted consequences, such
58 as additional building heave or settlement, potential for tensile axial stresses during pile
59 cooling, potential for large compressive axial stresses during heating, mobilization of
60 nonlinear deformations, or potential for thermally induced soil dragdown on the pile
61 (Laloui et al. 2006; Amatya et al. 2012; McCartney and Murphy 2017).

62 Thermal response tests (TRTs) are commonly used to estimate the thermal
63 properties of the energy pile and surrounding subsurface (Loveridge et al. 2020), but they

64 also provide an opportunity to characterize the thermo-mechanical response of the
65 energy pile (Murphy et al. 2015). As TRTs typically involve injection of heat into the
66 subsurface, they are particularly applicable in evaluating the conditions expected for
67 energy pile use in tropical climates that are cooling dominated. In a TRT, a heat exchange
68 carrier fluid is circulated through a closed-loop pipe, which may be embedded within an
69 energy pile or a borehole leading to heat transfer primarily by conduction (Gehlin et al.
70 2002). Data on the evolution in the inlet and outlet fluid temperatures along with the fluid
71 flow rate are acquired to understand the heat transfer rate into or from the subsurface,
72 while embedded sensors are used to monitor the changes in axial or radial strain.

73 Along these lines, several studies have investigated the impacts of temperature
74 changes on axial strains in energy piles (Laloui et al. 2006; Brandl 2006; Bourne-Webb
75 et al. 2009; McCartney and Murphy 2012; Akrouch et al. 2014; Mimouni and Laloui 2014;
76 Wang et al. 2014; Murphy et al. 2015; Sutman et al. 2015; Murphy and McCartney 2015;
77 McCartney and Murphy 2017; Faizal et al. 2018). It has been well established that
78 changes in temperature along the energy pile generate deformations that can cause
79 additional axial stresses depending on the restraint conditions, and these stresses must
80 be accounted for properly in energy pile design (Mimouni and Laloui 2014). Further,
81 increases in temperature may affect the soil-pile interface shear strength, either due to
82 thermal consolidation of saturated soils or thermally-induced drying of unsaturated soils.
83 For example, recent studies involving laboratory tests (Di Donna et al. 2016) and
84 centrifuge modeling (McCartney and Rosenberg 2011; Ng et al. 2014; Stewart and
85 McCartney 2014; Goode and McCartney 2015; Ghaaowd and McCartney 2018) have
86 investigated the impacts of soil on the thermo-mechanical response of energy pile.

87 Ghaaowd and McCartney (2018) found that the pullout capacity of energy piles in soft,
88 saturated clays increased significantly due to thermal consolidation of the soil near the
89 pile interface. McCartney and Rosenberg (2011) found that energy piles in unsaturated
90 silt heated from 15 to 60°C and then loaded axially to failure had a side shear resistance
91 that was 40% greater than that of baseline foundations tested at ambient temperature.
92 Goode and McCartney (2015) performed additional testing that confirmed these trends,
93 and Behbehani and McCartney (2020) found that these trends were due to an increase
94 in effective stress along the pile associated with thermally induced drying of soil near the
95 energy pile.

96 Several studies have investigated the effects of temperature on the interface
97 behavior between soils and structural elements. Di Donna et al. (2016) observed an
98 increase of the interface shear strength due to heating. Murphy and McCartney (2014)
99 performed thermal borehole shear tests and found no changes in the soil-concrete
100 interface frictional response with increased temperature, although changes in the
101 undrained interface shear strength may occur due to thermal consolidation or thermally
102 induced drying. Although the impact of cyclic heating and cooling on the volume change
103 and shear strength has been investigated through laboratory test and centrifuge modeling
104 (Di Donna et al. 2016; Vega and McCartney 2015), it is not well understood and studied
105 at field scale and this paper aims to show results from hysteresis on field scale
106 experiments. Mortara et al. (2007) evaluated the effect of the interaction between sand
107 and structural materials and concluded that for cyclic tests the densification produced a
108 gradual increase in the maximum shear stress during the cycles. Likewise, the final value

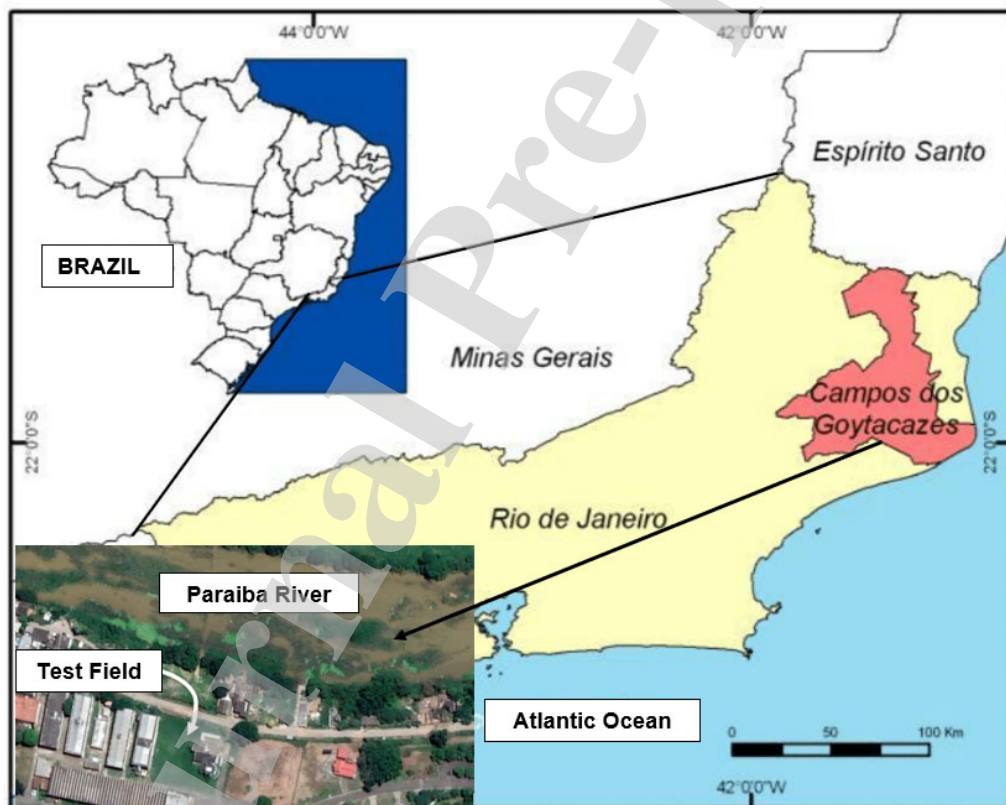
109 of shear stress for an interface depends on the amount of densification of the sand at the
110 interface due to cycling.

111 This study presents a field investigation involving cyclic thermal response tests on
112 an energy micropile, a small-diameter, drilled and grouted non-displacement pile whose
113 reinforcement cage is pushed into concrete after it is placed into the hole. Energy
114 micropiles have not been thoroughly investigated and may have different behavior than
115 typical bored piles that are thoroughly cleaned with placement of the reinforcement cage
116 before concrete placement. In particular, a potentially nonuniform cross-sectional
117 geometry with depth and a toe that may contain loose materials are two issues that may
118 affect thermo-mechanical soil-structure interaction in energy micropiles. For example,
119 Moradshahi et al. (2020) highlighted the potential impacts of poor cleanout of the toe on
120 the thermal soil-structure response of a typical bored pile. The case that they investigated
121 was an anomaly for a bored pile due to the poor cleanout, while micropiles routinely have
122 poor cleanout at the toe. This means that restraint for thermal expansion and contraction
123 is largely controlled by the side shear resistance in energy micropiles. Further, the cross-
124 sectional geometry may also vary with depth when an energy micropile is installed
125 through a stratified subsurface. This paper focuses on understanding the impact of
126 different soil layers on the thermo-mechanical response of an energy micropile in a
127 stratified soil layer using four thermal response tests. Specifically, these TRTs permit
128 characterization of the hysteretic response at different depths in the energy pile and were
129 also performed with different heat transfer rates, which helps understand the role of this
130 variable on the thermo-mechanical behavior.

131

132 Field Test Site

133 The field test site is located in Campos dos Goytacazes in the north of Rio de
134 Janeiro state, Brazil, on the margin of the Paraíba River at the coordinates $21^{\circ}45'38.4\text{S}$,
135 $41^{\circ}17'34.2''\text{W}$ as shown in Figure 1. The city has a tropical weather with winter dry season
136 and is classified as Aw according to the Köppen and Geiger weather classification
137 system. The city has an annual average temperature of 24.1°C reaching a maximum of
138 35°C during the summer.



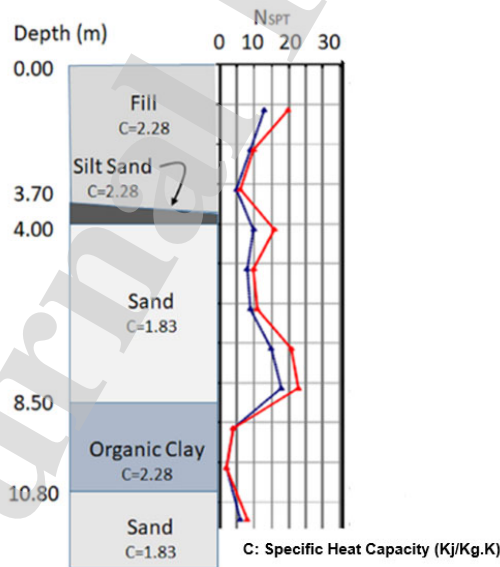
139

140

141

Figure 1 - Location of the site investigation.

142 A site investigation was performed in July 2017 extending 12 m below the ground surface.
 143 Exploration results from the borehole showed three prominent strata. The top layer is
 144 approximately 3.5 m-thick and consists of sandy-clay fill. Beneath the fill is a 1.5 m-thick
 145 silty-sandy layer, followed by a 3 m-thick layer of sand, which is assumed to be part of
 146 the Paraiba basin sediment. An organic clay layer was encountered between depths of
 147 8.50 and 10.80 m, underlain by a silty sand layer extending to the maximum depth
 148 explored. More detailed information on soil profile is shown in Figure 2. Based on the SPT
 149 blow counts shown in Figure 2, it is likely that the organic clay layer is relatively soft and
 150 can be assumed to be normally consolidated. Since the site is located near the Paraiba
 151 river the soil deposit experiences a significant seasonal ground water table Fluctuation.
 152 At the time of the site investigation the ground water table was at a depth of 6.5 m, so the
 153 organic clay layer can be assumed to be saturated.



154

155

Figure 2 - Soil strata and standard penetration test (SPT) blow counts.

156

157 **Experimental setup**

158 A 0.4 m-diameter energy pile was installed in sedimentary soil to a depth of 12 m
159 using procedures representative of micropiles. Specifically, the hole was drilled with an
160 auger, concrete was placed during auger extraction, and the reinforcing cage was placed
161 after auger extraction. The concrete used in the pile had a tensile strength of 3.4 MPa
162 and a compressive strength of 29 MPa measured from a diametric Brazilian test. The
163 foundation contains a 9.5 mm-diameter steel reinforcing cage configured in a triangular
164 arrangement that extends along the full length of the shaft. A loop of 25 mm-diameter
165 heat exchange tubing composed of PEX-A monolayer was installed in the pile and placed
166 in a "U" shape attached to the inside of the reinforcing cage (Fig. 3a).

167 The energy pile was equipped with four Geokon model 4150 vibrating wire strain
168 gauges attached to the reinforcing cage (Fig. 3b) at different locations along the length of
169 the pile which are shown in Fig 3a. The strain gauges and thermistors were attached to
170 the reinforcing cage so that their final positions would be at depths of 11.5 m (A05), 8.77
171 m (A04), 6.1 m (A03) and 3.2 m (A02). They were used to monitor the temporal and
172 spatial distributions with depth in temperature and axial strain during the heating and
173 cooling processes. The strain gauges and thermistor sensor cables were connected to a
174 Geokon data acquisition system (Fig 3c) allowing to monitor temperature and strain
175 variations on the energy foundation in 10 minutes intervals. Separately, pipe plug
176 thermistors were installed at the inlet and outlet of the heat exchange tubing loop at the
177 head of the pile to measure the inlet and outlet temperatures of the heat exchanger fluid
178 on the foundation,. The final configuration of the test consists of a water circulation pump,
179 a flow meter, a water heater that permits control of the input and thermally isolated water

180 tank as shown in Fig. 4b and 4c. The energy micropile studied is not restrained at the
181 head and is partially restrained at the bottom as the pile was not socketed into a stiff layer.
182 The micropile construction process and the small SPT blow count of the soil layer at the
183 toe of the pile (7 blows) indicates that the toe of the soil may experience deformations
184 during heating and cooling cycles. Accordingly, the energy micropile can be characterized
185 as a semi-floating energy pile whose main resistance to axial loading and thermal
186 expansion is from side shear resistance.

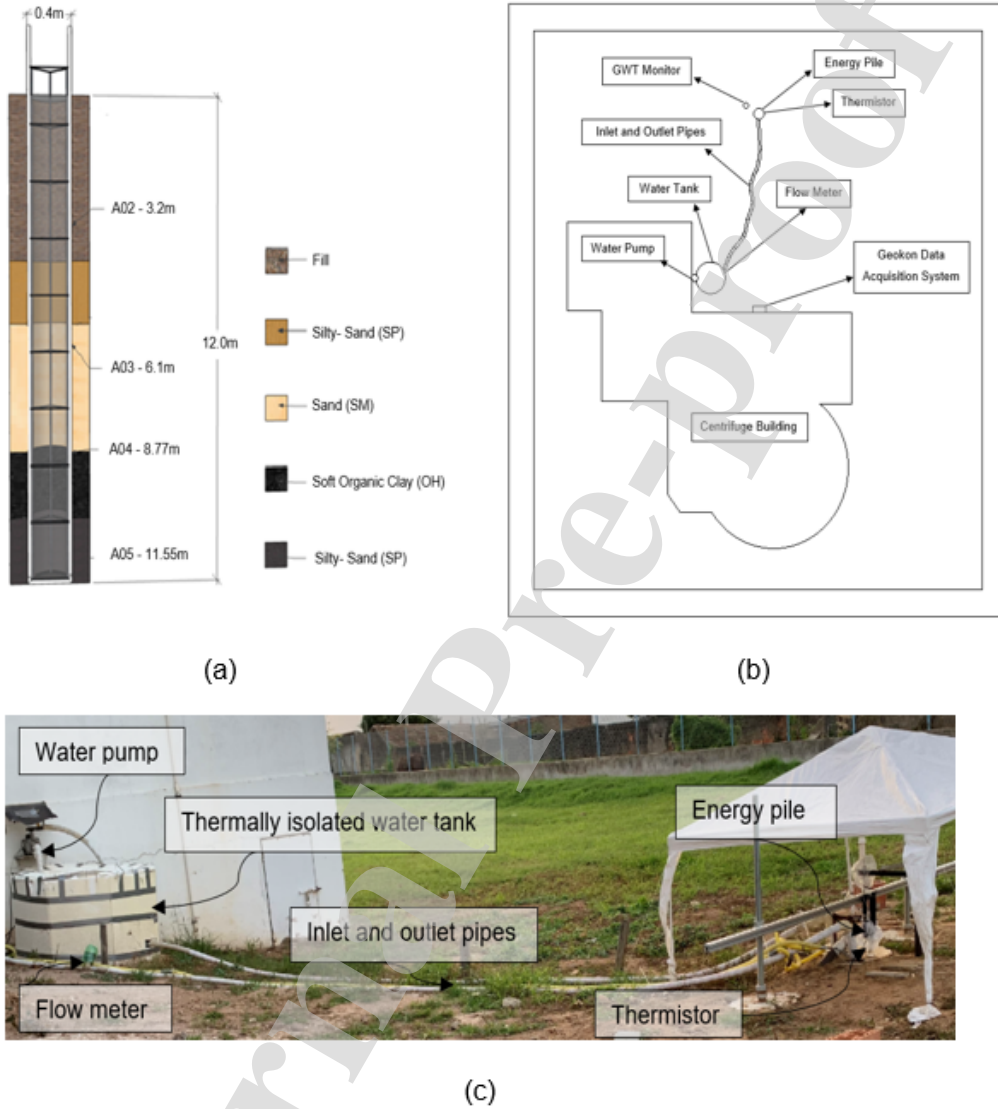
187



188

189 Figure 3 - Details of the heat exchange tube installation, strain gauge installation on a
190 reinforcing element, and Geokon data acquisition system.

191



192

193

194

195

Figure 4 – (a) Pile instrumentation scheme; (b) Schematic of the system used to perform the Thermal Response Tests (c) Photograph of the system.

196 **Test procedures**

197 A series of four thermal response tests (TRT) were carried out on the same energy pile,
 198 referred to as Reference TRT, TRT #1, TRT #2, and TRT #3, as summarized in Table 1.
 199 The first test carried out on the pile by Ferreira (2017) was used as a Reference Test.
 200 During the TRTs performed in this study, the inlet and outlet heat exchange fluid
 201 temperatures were continuously monitored. The heat exchange fluid flow rate was
 202 different in each of the tests, with a flow rate of 19.4 l/min in the Reference Tests, 30.1 l/min
 203 in the test #1, and a flow rate of 19.7 l/min in the tests #2 and #3. These flow rates
 204 correspond to a turbulent flow regime within the heat exchanger pipes. The Reference
 205 TRT was carried out with an inlet power source of 1.0 kW, TRTs #1 and 2 were executed
 206 with a heat transfer rate of 1.3 kW while TRT# 3 was executed with a heat transfer rate
 207 of 2.4 kW, allowing an evaluation of the effect of the pile and the surrounding soil when
 208 submitted to a higher temperature gradient.

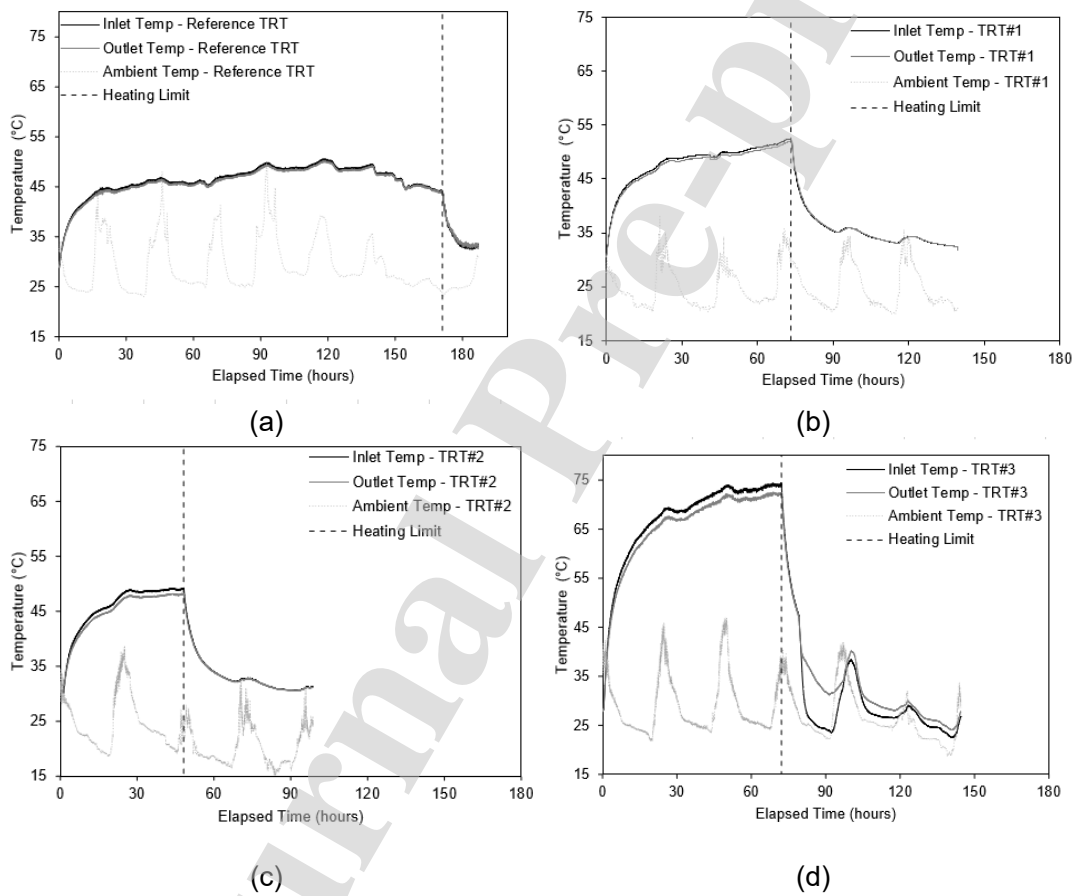
209 Table 1 - Summary of thermal response testing details.

TRT	Test end date	Heat exchanger fluid flow rate (l/min)	Inlet power source (W)	Approximate heating duration (hours)	Approximate increase in temperature (°C)
Reference TRT	09/2016	19.4	1000	171	13
TRT #1	06/2019	30.1	1300	75	14
TRT #2	08/2019	19.7	1300	50	12
TRT #3	09/2019	19.7	2400	75	22

210

211 The durations of heating in the four TRTs were 171, 75, 50 and 75 hours,
 212 respectively, and time series of pile temperatures during heating and cooling along with
 213 the ambient air temperatures during the tests are shown in Figure 5. The temperatures at
 214 different locations in the pile were found to be similar during each test. The average

215 increase in the water temperature recorded at the inlet and outlet of U-loop at the pile
 216 head during the Reference TRT, TRT#1, TRT#2 and TRT#3 were 13, 14, 12 and 22 °C,
 217 respectively. The ambient surface temperature only had a minor effect on the pile
 218 temperature, likely due to the effects of ambient surface temperature on the water storage
 219 tank used to supply the circulating water to the heater.



220

221 Figure 5 - Changes in pile temperature over time during the TRTs along with changes in
 222 the ambient surface temperature: (a) Reference TRT; (b) TRT#1; (c) TRT#2; (d) TRT#3.

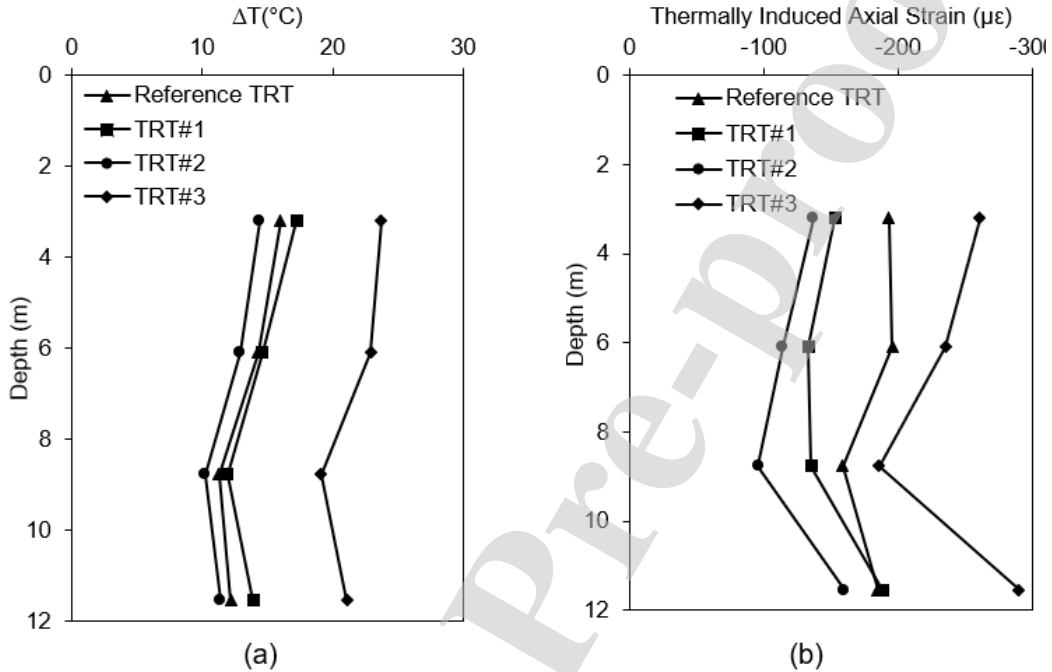
223 Analysis

224 As noted, energy piles expand axially during heating and thermally induced strains
 225 may be observed depending on the restraint provided by the overlying structure and the
 226 surrounding subsurface (Amatya et al. 2012). The thermal axial strains caused by heating
 227 were measured in this study using the vibrating wire strain gauges, installed inside the
 228 micropile, which were corrected for the local temperature effects recorded by co-located
 229 thermistors, as follows:

$$\varepsilon_{real} = B(R_1 - R_0) + (T_1 - T_0)\alpha_{steel} \quad (1)$$

230 where B is a constant strain gauge Batch Factor (0.962), R_1 and R_0 are the
 231 readings of the strain gauge at different times, and α_{steel} is the coefficient of linear thermal
 232 expansion of the vibrating steel wire in the strain gauges ($12 \mu\epsilon/^\circ\text{C}$) and T_1 and T_0 are the
 233 readings of strain gauge temperature at different times. The thermal axial strains
 234 calculated using Equation 1 are plotted versus depth in Figure 6a. The average
 235 temperature changes reached during TRT#1, TRT#2 and TRT#3 were 14, 12 and 22°C ,
 236 respectively. The thermal axial strains versus depth at the end of heating in each test,
 237 including the reference TRT, are shown in Figure 6b. Smaller thermal strains and
 238 temperatures are observed in each test at a depth of 9 m, possibly due the presence of
 239 the organic clay layer. Higher thermal strains are observed near the toe and the head of
 240 the energy pile in all three TRTs, which can be attributed to the high degree of freedom
 241 of the semi-floating pile in these locations. Specifically, the micro-pile was not connected
 242 to a superstructure, so it is free to move upward, and the construction approach used in
 243 micropiles leads to a considerable disturbance of the soil in the bottom boundary so it is

244 relatively free to move downward. The highest thermal axial strains were observed in
 245 TRT#3 due to the higher temperature applied in this test.



246 Figure 6 -(a) Profiles of temperature change; (b) Profiles of thermally induced strain.

247

248 When an energy pile is heated without restraint, it tends to expand freely with free
 249 thermal axial strains calculated as follows:

$$\epsilon_{t-free} = (T_1 - T_0)\alpha_{concrete} \quad (2)$$

250 where $\alpha_{concrete}$ is the coefficient of thermal expansion of reinforced concrete. However, an
 251 energy pile in the ground will not be able to expand freely, owing to mobilization of side
 252 shear restraint at the pile–soil interface and possible restraint at the pile head or toe.
 253 Accordingly, the measured strain changes due to temperature change ($\epsilon_{T-Observed}$) will
 254 be less than that given by Equation (2). The restrained strain ($\epsilon_{T-Restrained}$) creates

255 thermal stress in the pile and should be considered in structural design. The restrained
 256 axial strain can be estimated as (Knellwolf et al. 2011; Amatya et al. 2012):

$$\varepsilon_{T-Restrained} = \varepsilon_{T-Free} - \varepsilon_{T-observed} \quad (3)$$

257 The profiles of thermally induced strain and free thermal strain (i.e., the strain
 258 present if there is no soil restraint) are shown in **Error! Reference source not found.**
 259 The maximum strain occurred at about mid-depth, reflecting a semi-floating energy pile
 260 described by Amatya et al. (2012). A comparison of the measured strain profiles and the
 261 free thermal strain profile shows that the differences between these profiles change with
 262 each subsequent heating-cooling cycle. In the Reference TRT, the thermal strain
 263 mobilized was almost 90% of the free thermal strain at both ends, while about 75% was
 264 mobilized at the depth of 8.77 m. In TRT#3 around 72% of the thermal strain was
 265 mobilized at the ends while about 53% at the mid-depth. This indicates that over the
 266 cycles of heating, a decrease in the mobilized strains in the pile of about 20% was
 267 observed. This is potentially due to a gradual increase in stiffness of the ground with
 268 each test, with the changes mainly attributed to temperature effects, more pronounced
 269 on the organic clay layers. The minimum value of $\varepsilon_{T-Observed}$ is expected to decrease with
 270 increasing interface resistance and depends on a number of factors including the type of
 271 ground (clayey, granular), ground stiffness, groundwater level and the magnitude of heat
 272 input (Amatya et al. 2012). This observation can be noticed by analyzing results from the
 273 Reference TRT, TRT#1 and TRT#2 (Figure 7. a, b and c) performed with a similar
 274 average on temperature gradient, showing smaller values of $\varepsilon_{T-Observed}$ for the
 275 temperature gradient imposed during each tests.

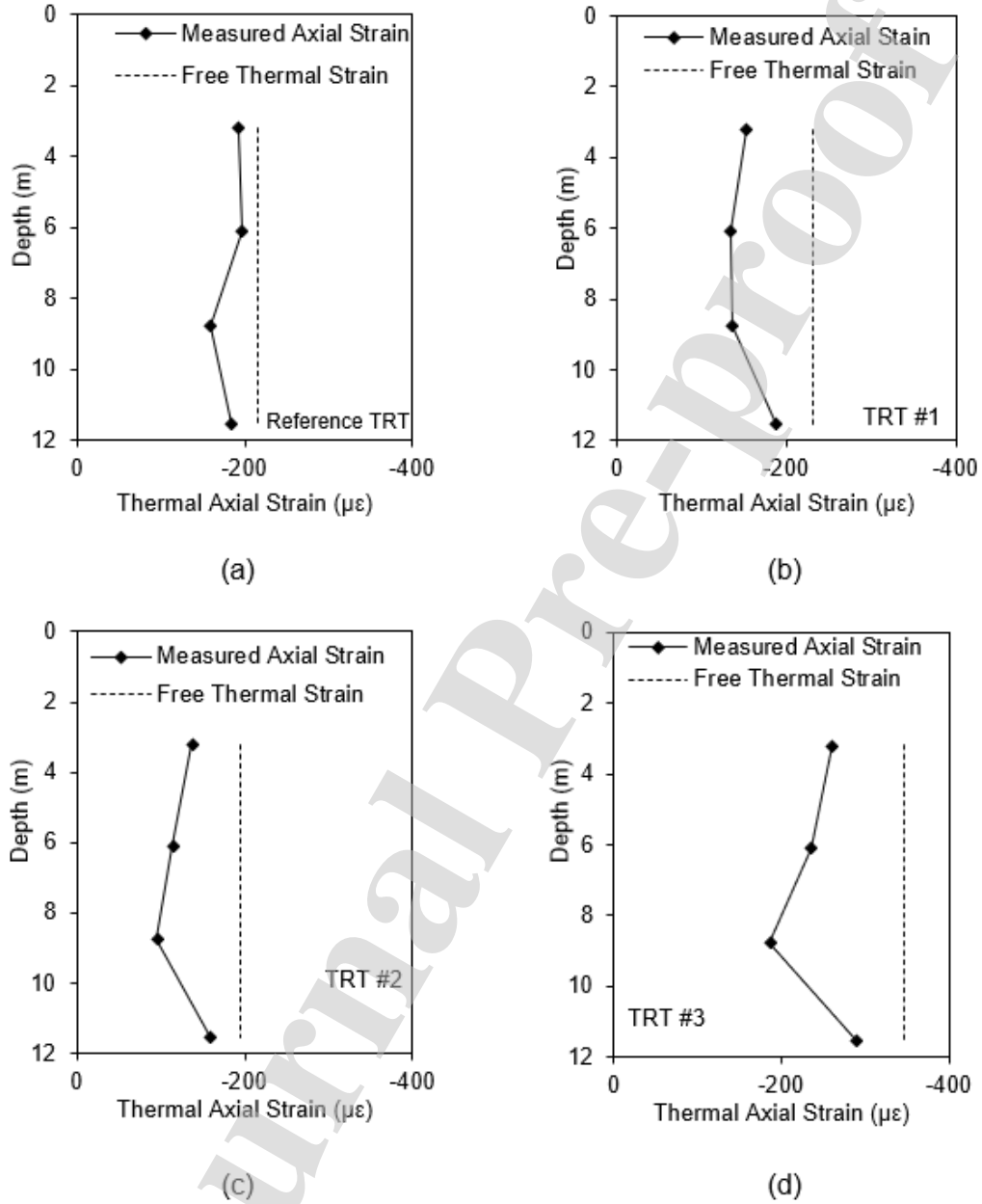
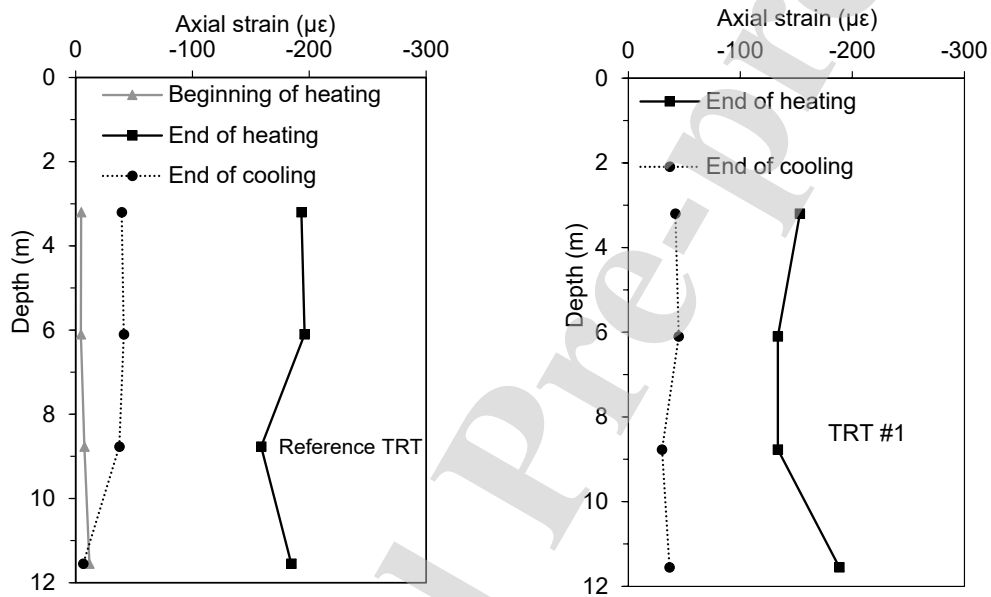
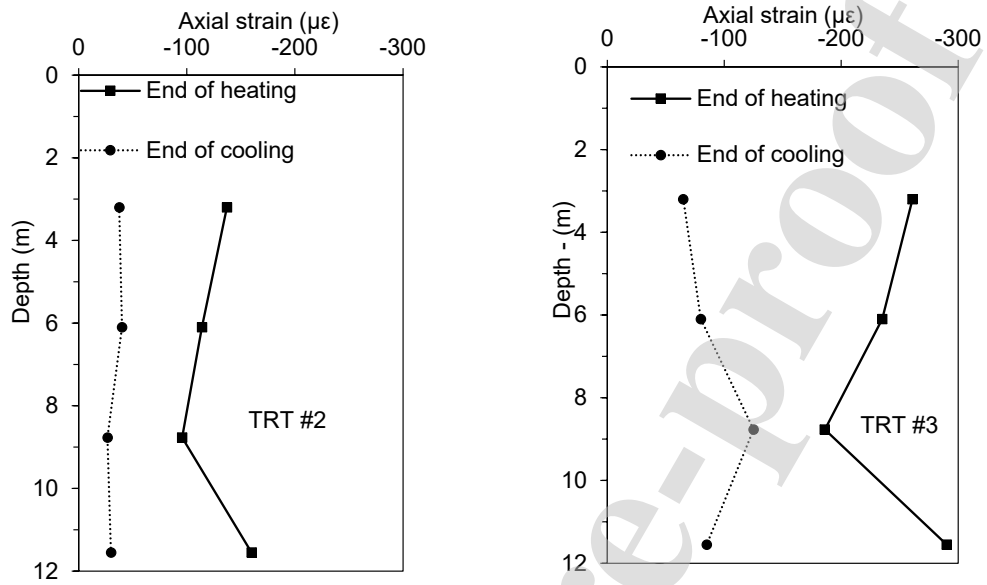


Figure 7 - Observed and free thermal strain profiles due to uniform heating with depth in the energy pile.

276 A comparison between thermal axial strain profile during heating and cooling for
277 the four TRTs is shown in Figure 8, where the thermal axial strain was zeroed at the
278 beginning of each test to show the differences in profiles at the end of heating and the
279 end of cooling. The thermal axial strains during heating are slightly different due to the
280 different imposed temperature gradients. Comparing the first 3 tests (Reference TRT,
281 TRT#1 and TRT#2), in which the imposed temperature gradient was similar, the thermal
282 axial strains during cooling returned to the values that were experienced before heating,
283 indicating linear thermo-elastic behavior, meaning permanent thermo-plastic
284 deformations did not occur in the energy pile-soil system, and consequently hysteresis
285 can be neglected. On the other hand, data from the third test (TRT#3), in which a higher
286 temperature gradient was imposed on the energy pile, approximately 50% higher than
287 the temperature imposed on the first three cycles, it is possible to notice that irreversible
288 strains on the clay-concrete interface. This is better highlighted in the comparison of
289 thermal axial strains in (Figure 9). This indicates that permanent thermo-plastic
290 deformations occur at the Interface between the energy pile and the organic clay
291 interface, possibly indicating that the mobilized side shear resistance during the heating
292 test lead to locked-in plastic strains at the interface. It should be noted that irreversible
293 strains were observed during a thermal cycle in which a higher thermal load was imposed,
294 meaning that at a certain temperature, the yield surface was expanded and thermal
295 plastic deformations occurred in the clay layer beyond that experienced during the
296 Reference TRT and the other two TRTs. After thermal plastic deformations, soils a lower
297 void ratio and a higher undrained shear strength which will result in more restraint to

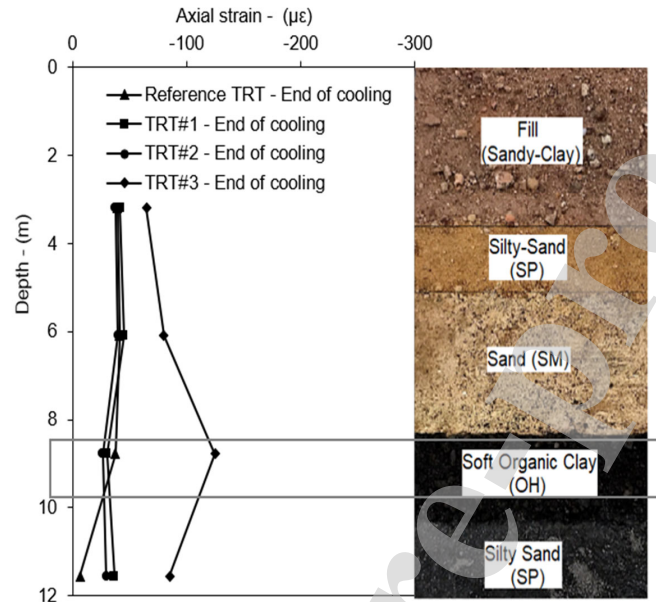
298 thermal expansion of the pile. That would explain why the mechanical responses of the
299 pile during the first 3 tests are quite similar, suggesting that the stage after maximum
300 heating is sufficient for the organic clay to return to the conditions induced by the initial
301 heating during Reference TRT.





302 Figure 8 - Thermal axial strain profiles during different stages of the TRTs.

303



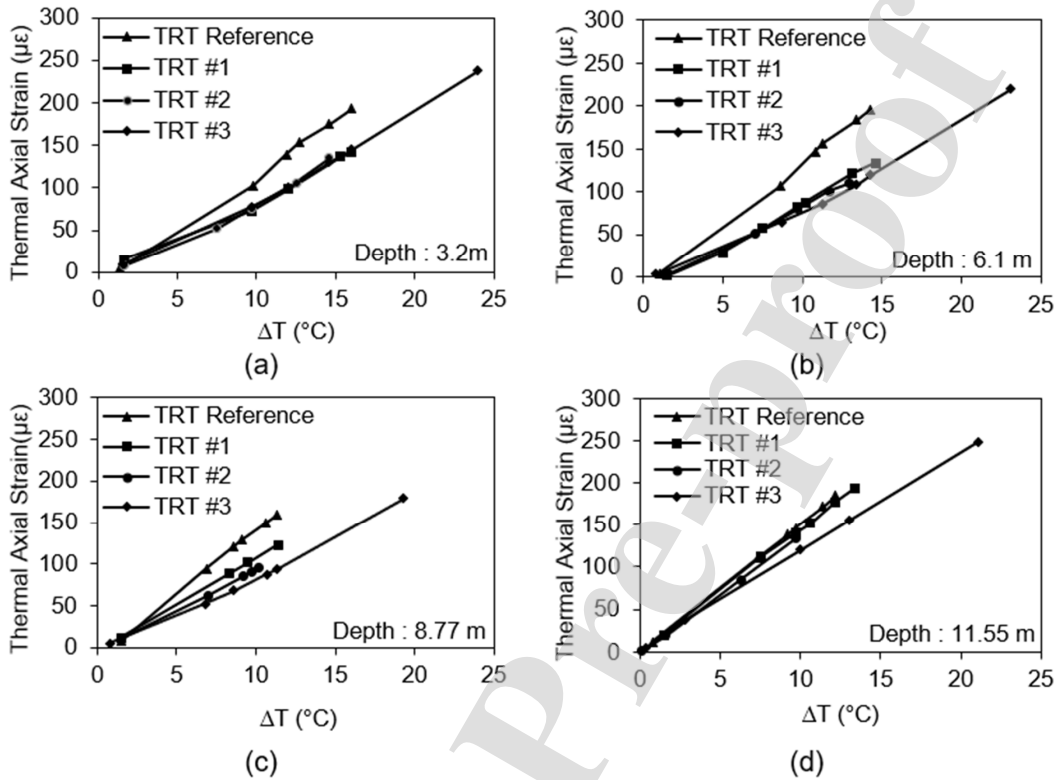
304

305 Figure 9 - Comparison of thermal axial strain profiles at the end of cooling for all TRTs.

306

307 Relationships between the thermal axial strain and the change in temperature for
 308 each depth in each test are shown in Figure 10a to Figure 10d. The slopes of each
 309 relationship correspond to the mobilized coefficient of thermal expansion. A linear
 310 relationship between the thermal axial strain and changes in temperature is noticed,
 311 similar to the behavior for an energy pile in sandstone reported by Murphy et al. (2015).
 312 At a depth between 8,77 and 11.55m (Figure 10c e 10d) correspond to the organic soft
 313 clay layer followed by a clean sand layer the slopes of the curves were observed to
 314 decrease with changes in temperature reflecting an increase in interface shear strength..
 315 Similar behavior has been reported by Di Donna et al. (2015), who tested the response
 316 of clay-concrete interfaces at different temperatures after cyclic heating and cooling, and
 317 also by Ghaaowd and McCartney (2018) who performed pullout tests on energy piles

318 after a heating-cooling cycle. Conversely, for the sensors located at depths of 3.2m in the
319 fill layer composed mostly of sand (Figure 10a) and at a depth of 6.1 m in the sand layer
320 (**Error! Reference source not found.**b), heating led to a negligible change in behavior.
321 This behavior was observed by Goode and McCartney (2015) during heating semi-
322 floating energy piles in dry sand and by Di Donna et al. (2015) during application of
323 temperature cycles to a sandy soil pile interface. Overall, the results in Figure 10 indicate
324 that when an energy pile is installed in a stratified soil layer that the effects of temperature
325 on each soil layer should be carefully assessed, as the axial strains within each of the
326 layers had a different variation with each TRT. The reduction in thermal axial strain with
327 changes in temperature indicates an increase in resistance of the soil layers to thermal
328 expansion. Moreover, the changes in behavior at a certain depth will have an influence
329 on the profile of thermal axial strain after several cycles of heating and cooling. This may
330 indicate that interface shear testing similar to Di Donna et al. (2015) should be performed
331 for the different layers in a stratified soil deposit



332

333

334

335

336

337

338

339

340

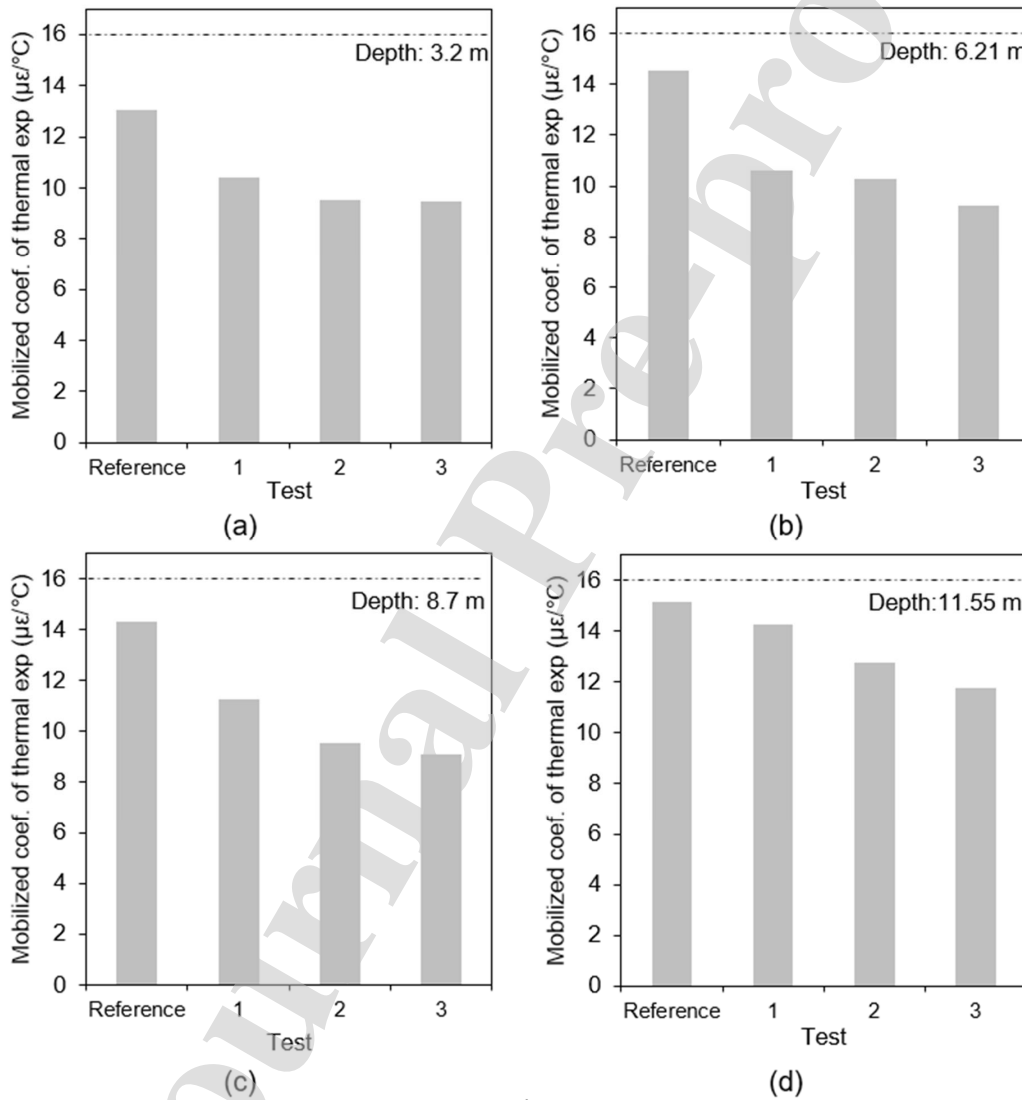
341

342

Figure 10 - Relationships between the thermal axial strain and the change in temperature at different depths along the energy pile: (a) 3.2 m; (b) 6.1 m; (c) 8.77 m; (d) 11.55 m.

The mobilized coefficients of thermal expansion for the depth of each strain gage during each test are plotted in Figure 11. The increase in each test temperature is shown in Table 1. In all cases, the values of the mobilized coefficient of thermal expansion decreased after each subsequent heating cycle, reflecting smaller displacements throughout the pile with temperatures increments. This behavior can be associated with an increase in side shear resistance along at the length of the pile due to heating. It is

343 possible that thermally induced drying led to an increase in restraint in these tests as
 344 observed by Behbehani and McCartney (2020), but also could be related with thermal
 345 consolidation of the softer clay layer that results in greater restraint.



346

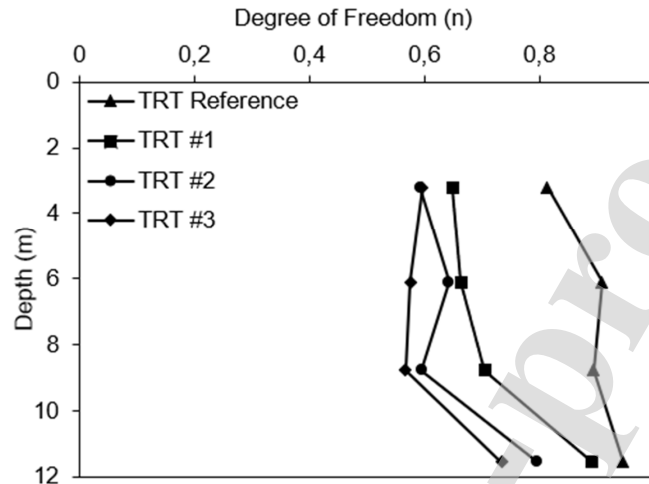
347 Figure 11 - Mobilized coefficients of thermal expansion measured in each test at
 348 different depths along the energy pile: (a) 3.2 m; (b) 6.1 m; (c) 8.77 m; (d) 11.55 m.

349

350 The effects of heating of the energy micropile on the surrounding soil layers were
351 found to be not negligible. To better interpret this behavior, it is interesting to understand
352 the degree of freedom of the pile defined by the ratio between the free and observed axial
353 strains, ε_{T-free} and $\varepsilon_{T-observed}$ (Knellwolf et al. 2011).

$$DOF = \frac{\varepsilon_{T-free}}{\varepsilon_{T-observed}} \quad (4)$$

354 The degree of freedom is theoretically zero when the pile is fully restrained
355 (blocked) and 1 when the pile is completely free to move. Generally, it ranges from zero
356 to 1 because of the variable shaft friction mobilization and restraint at the two extremities
357 of the pile (Knellwolf et al. 2011). The values of degree of freedom along the pile length
358 achieved in all tests are shown in Figure 12. The minimum pile restraint is observed at a
359 depth of 11.55 m, corresponding to points of maximum strain located near the energy pile
360 toe. This is, likely due to the lower amount of restraint provided by the deepest soil layer
361 and the low end bearing capacity expected for the micropile construction technique used
362 for the pile on the grounds of a low end bearing capacity provided by this foundation.
363 According to Brandl (2006) the pile installation has a great influence on the geotechnical
364 performance of energy piles. Conversely, maximum pile restraint was observed at a depth
365 of 8-10 m, corresponding to the location of the minimum thermal axial strain as a result
366 of the presence of the organic clay layer. From the Reference TRT to the last TRT
367 (TRT#3) a reduction of around 0.25 in the degree of freedom of the pile is observed. The
368 rate of increase in the degree of freedom from test to test was about 60% at the toe of
369 the pile and 29% at the head of the pile which shows an increase in the restraint provided
370 by the surrounding soil over the four heating tests.



371

372

Figure 12 - Variations of degree of freedom along the pile for each TRT.

373

374

375

376

377

378

379

380

381

382

383

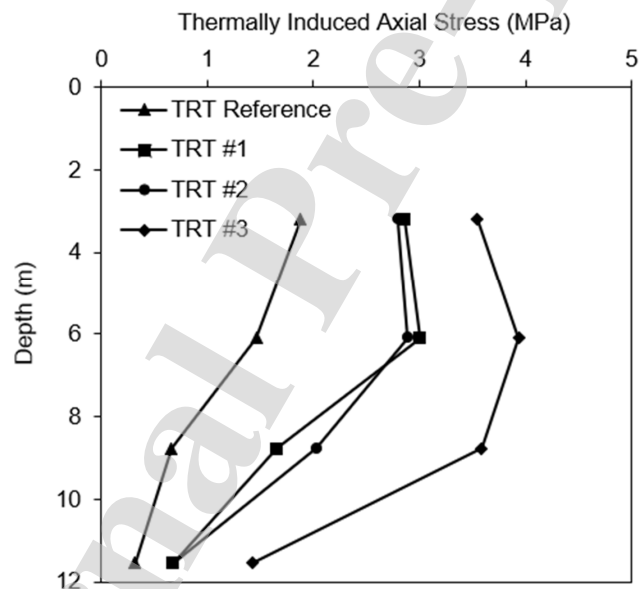
384

385

386

Because of the values of restrained strain and decreasing degree of freedom with each test, significant thermal axial stresses are induced by thermal loading that increase in each test are induced in the energy micropile and should be considered in structural design. Thermally induced axial pile stress change is a function of the restrained boundary condition of the pile, which is determined mainly by the lateral confining pressure and change in temperature. The thermal axial stress during each TRT shown in Figure 13 indicate that the development of axial stress is larger over the mid-length of the pile. This verifies the hypotheses of Bourne-Webb et al. (2012) and Amatya et al. (2012) that during heating the maximum thermally induced axial stress of a semi-floating energy pile should be near the mid-length of the pile. Further, the minimum thermal induced axial stress is located near the bottom portion of the pile at the depth of 11.5 m in all TRTs, whereas the maximum strain was observed at the toe which means that the end bearing resistance provides small resistance that may increase over several cycles of heating and

387 cooling. A maximum thermal induced axial stress of about 2 MPa during a change in
 388 temperature of 13 C° was developed at a depth of 3.2 m. This depth lies within the sandy
 389 layer and represents the depth providing the maximum side shear restraint. On the other
 390 hand, in the last TRT (TRT #3) the maximum thermal induced axial stress of about 4 MPa
 391 observed during a change in temperature of 22 C° occurred at a depth of 6.1m. This depth
 392 also lies within the sandy layer but indicates that hysteretic heating-cooling cycles
 393 contribute to a gradual change in the location of maximum thermal axial stress.



394

395 Figure 13 - Thermally induced axial stresses along the pile in each test.

396

397 Conclusion

398 Three thermal response tests were performed on a cast-in-place energy micropile
 399 in a stratified sedimentary soil layer typical of tropical regions to study the effects of
 400 heating and cooling cycles beyond a reference test performed in an earlier study. Due to

401 different heat exchanges process in each test, an increase in the change in temperature
402 was imposed in each test which permits thermal plasticity effects to be observed. The
403 overall conclusions from this field study are that the construction techniques that greatly
404 disturb the soil at the pile base and the soil stratigraphy with the presence of organic clay
405 can cause considerable changes in thermo-mechanical soil structure interaction during
406 cycles of heating and cooling. The following specific comments can be drawn:

- 407 • The energy micropile with no head load behaved like a semi-floating energy pile
408 with maximum thermal axial strains near to the head and toe of the pile due to the
409 micropile construction technique that leaves losing material near the end of the
410 pile.
- 411 • The presence of an organic clay layer in the bottom half of the energy pile was
412 found to have a major effect on the energy pile restraint, with the lowest thermal
413 axial strains encountered at this depth. Although the thermal axial strains after
414 cooling were similar for the Reference TRT and the first two TRTs performed in
415 this study, the greater change in temperature during the third TRT led to permanent
416 strains after heating which indicates thermo-plastic behavior in the organic clay
417 layer induced by heating.
- 418 • A linear change in thermal axial strain with changes in temperature was observed
419 for all depths indicating thermo-elastic response of the energy pile during several
420 cycles of heating and cooling.
- 421 • The mobilized coefficients of thermal expansion changed during each test,
422 possibly due to changes in side shear restraint and changes in the end bearing
423 resistance. It reached the highest values in locations of maximum strain near the

424 energy pile toe due to the lower restraint associated with the micropile construction
425 technique, although this increased with each cycle. Conversely, the lowest values
426 of the mobilized coefficient of thermal expansion corresponded to the location of
427 the minimum thermal axial strain in the organic clay layer.

428

429 **Acknowledgments**

430 The Authors are grateful to CNPQ (Brazilian Research Council) and the Rio de Janeiro
431 Research Foundation Grant - FAPERJ for the scholarship of the first Author.

432

433 **References**

- 434 Akrouch, G., Sánchez, M. & Briaud, J.-L. (2014). Thermo-mechanical behavior of energy
435 piles in high plasticity clays. *Acta Geotechnica*. 9(3): 399-412.
- 436 Amatya, B.L., Soga, K., Bourne-Webb, P.J., Amis, T. & Laloui, L. (2012). Thermo-
437 mechanical behaviour of energy piles. *Géotechnique*. 62(6): 503-519.
- 438 Bourne-Webb, P.J., Amatya, B., Soga, K., Amis, T., Davidson, T. & Payne, P. (2009).
439 Energy pile test at Lambeth College, London: geotechnical and thermodynamic
440 aspects of pile response to heat cycles. *Géotechnique*, 59(3): 237-248.
- 441 Brandl, H. (2006). Energy foundations and other thermo-active ground structures.
442 *Géotechnique*, 56(2): 81-126.
- 443 Chen, D. & McCartney, J.S. (2016). Parameters for load transfer analysis of energy piles
444 in uniform non-plastic soils. *ASCE International Journal of Geomechanics*.
445 04016159-1-17.10.1061/(ASCE)GM.1943-5622.0000873.

- 446 Di Donna, A. & Laloui, L. (2013). Advancements in the geotechnical design of energy
447 piles. Proceedings of International Workshop on Geomechanics and Energy,
448 Lausanne, Switzerland, pp. 26–28.
- 449 Di Donna, A. & Laloui, L. (2015). Numerical analysis of the geotechnical behaviour of
450 energy piles. *Int. J. Numer. Analyt. Methods Geomech.* 39, No. 8, 861-888.
- 451 Di Donna, A., Ferrari, A. & Laloui, L. (2016). Experimental investigation of the soil
452 concrete interface: physical mechanisms, cyclic mobilization and behavior at
453 different temperatures. *Can. Geotech. J.* 53(4): 659–672.
- 454 Faizal, M., Bouazza, A., Haberfield, C. & McCartney, J.S. (2018). Axial and radial thermal
455 responses of a field-scale energy pile under monotonic and cyclic temperature
456 changes. *Journal of Geotechnical and Geoenvironmental Engineering, ASCE,*
457 144(10): 04018072.
- 458 Ferreira, M.S. (2017). Estacas geotérmicas: uso de energia sustentável e resposta
459 termomecânica sob variação de temperatura. Dissertação de Mestrado.
- 460 Gehlin, S. (2002). Thermal Response Test: Method Development and Evaluation.
461 Doctoral Thesis. Lulea - Norrbotten, Suécia, Luleå University of Technology.
- 462 Ghaaowd, I. & McCartney, J.S. (2018). Centrifuge modeling of temperature effects on the
463 pullout capacity of energy piles in clay. DFI 43rd Annual Conference on Deep
464 Foundations. Anaheim, CA. Oct 24-27. 1-7.
- 465 Mortara, G. Mangiola, A., and Ghionna, V.N. (2007). Cyclic shear stress degradation and
466 post-cyclic behaviour from sand–steel interface direct shear tests. *Canadian*
467 *Geotechnical Journal.* 44(7): 739-752. <https://doi.org/10.1139/t07-019>

- 468 Knellwolf, C., Peron, H., & Laloui, L. (2011). Geotechnical analysis of heat exchanger
469 piles. *Journal of Geotechnical and Geoenvironmental Engineering*, ASCE,
470 137(10), 890-902.
- 471 Laloui, L. Nuth, M., & Vulliet, L. (2006). Experimental and numerical investigations of the
472 behaviour of a heat exchanger pile. *International Journal for Numerical and*
473 *Analytical Methods in Geomechanics*, 30: 763-781.
- 474 McCartney, J.S. & Rosenberg, J.E. (2011). Impact of heat exchange on the axial capacity
475 of thermo-active foundations. In: Han J., Alzamora D.E. (eds) *Proc. Geo-Frontiers*
476 2011 (GSP 211). ASCE, Reston VA, pp 488-498.
- 477 McCartney, J.S. & Murphy, K.D. (2012). Strain distributions in full-scale energy
478 foundations. *DFI Journal*. 6,(2): 26-38.
- 479 McCartney, J.S. & Murphy, K.D. (2017). Investigation of potential dragdown/uplift effects
480 on energy piles. *Geomechanics for Energy and the Environment*, 10(June): 21-28.
- 481 Mimouni, T. & Laloui, L. (2014). Towards a secure basis for the design of geothermal
482 piles. *Acta Geotechnica*. 9(3): 355–366.
- 483 Murphy, K.D. & McCartney, J.S. (2014). Thermal borehole shear device. *ASTM*
484 *Geotechnical Testing Journal*. 37(6), 1040-1055.
- 485 Murphy, K.D., McCartney, J.S. & Henry, K.S. (2015). Evaluation of thermo-mechanical
486 and thermal behavior of full-scale energy foundations. *Acta Geotechnica* 10(2):
487 179-195.
- 488 Sutman, M., Olgun, C.G., & Laloui, L. (2019). Cyclic load–transfer approach for the
489 analysis of energy piles. *Journal of Geotechnical and Geoenvironmental*
490 *Engineering* 145(1): 04018101.

- 491 Vega, A. & McCartney, J.S. (2015). Cyclic heating effects on thermal volume change of
492 silt. *Environmental Geotechnics*. 2(5), 257-268.
- 493 Wang, B., Bouazza, A., Singh, R. M., Haberfield, C., Barry-Macaulay, D. & Baycan, S.
494 (2014). Post temperature effects on shaft capacity of a full-scale geothermal
495 energy pile. *J. Geotech. Geoenviron. Engng* 141(4): 04014125.
- 496 Yavari, N., Tang, A. M., Pereira, J.M. & Hassen, G. (2016). Effect of temperature on the
497 shear strength of soils and soil/ structure interface. *Can. Geotech. J.* 53(7): 1186-
498 1194.
- 499
- 500
- 501